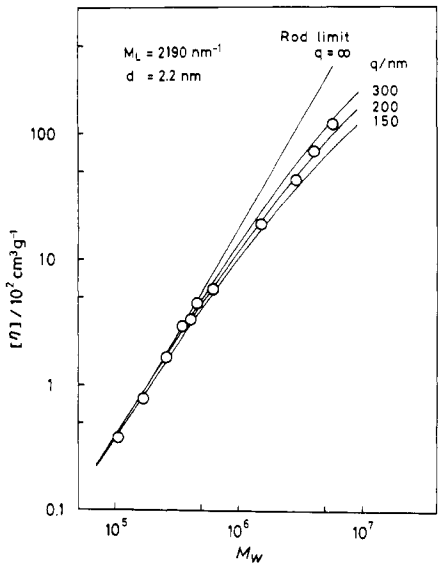

Figure 10. Comparison of the measured $[\eta]$ for schizophyllan in 0.01 N NaOH with Yamakawa and Yoshizaki's theoretical values for wormlike cylinders calculated for q = 150, 200, 300 nm, and ∞ with M_L and d fixed at 2190 nm^{-1} and 2.2 nm, respectively.

schizophyllan in water,[4] the model triple helix of schizophyllan,[3] and triple helices of other polysaccharides[17–19] in the crystalline state. Our pitches from light scattering and viscosity in 0.01 N NaOH agree not only with Yanaki et al.'s values[4] from sedimentation velocity and viscosity but also with the value estimated from the molecular model for schizophyllan. They are also close to the values for a β-1,3-D-xylan,[17] lentinan (β-1,3-D-glucan),[18] and curdlan (β-1,3-D-glucan),[19] leading to the conclusion that the triple-helical structure of schizophyllan in 0.01 N NaOH and water is very similar to that of these other polysaccharides in the crystalline state.

Acknowledgment. We acknowledge with thanks a Grant-in-Aid for Scientific Research from the Ministry of Education. Thanks are extended to Taito Co. for the schizophyllan samples and a grant.

References and Notes

(1) Kikumoto, S.; Miyajima, T.; Yoshizumi, S.; Fujimoto, S.; Kimura, K. *J. Agric. Chem. Soc. Jpn.* **1970**, *44*, 337.
(2) Kikumoto, S.; Miyajima, T.; Kimura, K.; Okubo, S.; Komatsu, N. *J. Agric. Chem. Soc. Jpn.* **1971**, *45*, 162.
(3) Norisuye, T.; Yanaki, T.; Fujita, H. *J. Polym. Sci., Polym. Phys. Ed.* **1980**, *18*, 547.
(4) Yanaki, T.; Norisuye, T.; Fujita, H. *Macromolecules* **1980**, *13*, 1462.
(5) Yamakawa, H.; Fujii, M. *Macromolecules* **1973**, *6*, 407.
(6) Yamakawa, H. *Macromolecules* **1975**, *8*, 339.
(7) Yamakawa, H.; Yoshizaki, T. *Macromolecules* **1980**, *13*, 633.
(8) Berry, G. C. *J. Chem. Phys.* **1966**, *44*, 4550.
(9) Deželić, Gj.; Vavra, J. *Croat. Chim. Acta* **1966**, *38*, 35.
(10) Rubingh, D. N.; Yu, H. *Macromolecules* **1976**, *9*, 681.
(11) Einaga, Y.; Miyaki, Y.; Fujita, H. *J. Soc. Rheol. Jpn.* **1977**, *5*, 188.
(12) Einaga, Y.; Miyaki, Y.; Fujita, H. *J. Polym. Sci., Polym. Phys. Ed.* **1979**, *17*, 2103.
(13) Benoit, H.; Doty, P. *J. Phys. Chem.* **1953**, *57*, 958.
(14) Kratky, O.; Porod, G. *Recl. Trav. Chim. Pays-Bas* **1949**, *68*, 1106.
(15) Utiyama, H.; Sakato, K.; Ikehara, K.; Setsuiye, T.; Kurata, M. *Biopolymers* **1974**, *12*, 53.
(16) Godfrey, J. E.; Eisenberg, H. *Biophys. Chem.* **1976**, *5*, 301.
(17) Atkins, E. D. T.; Parker, K. D.; Preston, R. D. *Proc. R. Soc. London, Ser. B* **1969**, *173*, 209. Atkins, E. D. T.; Parker, K. D. *J. Polym. Sci., Part C* **1969**, *28*, 69.
(18) Bluhm, T. L.; Sarko, A. *Can. J. Chem.* **1977**, *55*, 293.
(19) Deslandes, Y.; Marchessault, R. H.; Sarko, A. *Macromolecules* **1980**, *13*, 1466.

Development of a Linear Helical Conformation from Its Cyclic Correlate. β-Spiral Model of the Elastin Poly(pentapeptide) $(VPGVG)_n$

C. M. Venkatachalam and D. W. Urry*

Laboratory of Molecular Biophysics and the Cardiovascular Research and Training Center, University of Alabama in Birmingham, Birmingham, Alabama 35294.
Received January 7, 1981

ABSTRACT: Mathematical methods of obtaining linear helical correlate structures from a given cyclic conformation are applied to the case of the linear poly(pentapeptide) poly(L-Val-L-Pro-Gly-L-Val-Gly), $(VPGVG)_n$, of elastin, leading to the derivation of low-energy β-spiral models of the polymer from the known structure of its cyclic correlate, *cyclo*-$(VPGVG)_3$.

The relevance of studies on cyclic peptides from the standpoint of biomolecular conformation and function is well reviewed.[1] The interest in cyclic peptides has been additionally enhanced by a recent proposal[2] that they may, in some cases, serve as instructive models for *linear* helical peptides. By small changes in torsion angles of a cyclic peptide, an acceptable linear conformation can be obtained. Thus one can expect to find linear sequential polymers having conformational features similar to those of the cyclic molecules with the same sequence. The linear and the "corresponding" cyclic molecules may then be viewed as "correlates" of each other. This idea, referred to as cyclic conformations with linear conformational correlates,[2] has recently found a fascinating application in the conformational studies of oligopeptides with the pentamer repeat sequence L-Val-L-Pro-Gly-L-Val-Gly, VPGVG, which is found in tropoelastin.[3–5] For instance, a detailed study[6] on the series of cyclic peptides *cyclo*-$(VPGVG)_n$, with n = 1–6, shows that *cyclo*-$(VPGVG)_3$ has NMR spectral properties strikingly similar to those of the linear polymer, $(VPGVG)_n$. The solid-state conformation of *cyclo*-$(VPGVG)_3$ has been determined by X-ray diffraction,[7] and the conformation in solution has been inferred from the combined analyses of NMR studies and

0024-9297/81/2214-1225$01.25/0

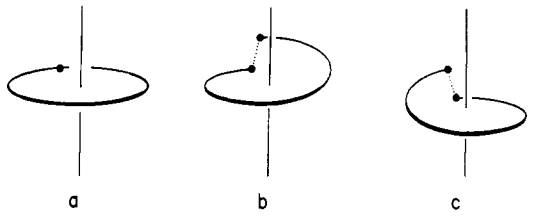

Figure 1. Schematic diagrams illustrating the "break opening" of a cyclic structure in (a) to obtain either a right-handed (b) or a left-handed correlate (c) with similar secondary structural features. The dot in (a) shows where the cyclic structure is opened enough to have sufficient end-to-end separation in (b) and (c) to relieve repulsive interactions. It is of interest to determine the relative stabilities of (b) and (c).

conformational energetics[8] to be quite similar to that found in the crystal. With the conformation of this cyclic correlate, *cyclo*-(VPGVG)$_3$, of the linear polypentapeptide well delineated, we have arrived at the interesting prospect of (1) starting from the known structure of *cyclo*-(VPGVG)$_3$, (2) going linear by "breaking open" the cyclic system, utilizing small changes in the torsion angles, and (3) deducing an acceptable low-energy conformation for the linear polypeptide, (VPGVG)$_n$.

In this short report, we employ the mathematical methods of deriving a linear helical conformation from its cyclic correlate for the cyclic correlate *cyclo*-(VPGVG)$_3$ and obtain low-energy helical conformations of linear (VPGVG)$_n$.

Energetics of the Linear Correlate

Since only minor changes in the torsion angles are needed on opening a stable and unstrained cyclic structure to obtain a linear correlate, it follows that the linear peptide with the same number of residues as in the cyclic molecule will likely have a minimum energy structure close to that of the cyclic structure. Of course, many other favorable structures can exist for the linear chain and one cannot state, without experimental demonstration of linear and cyclic correlates, that the energy-minimum correlate structure will always prevail over the other alternative structures that may be available for the linear chain. On the other hand, in the absence of any other data on the linear chain, the experimentally determined low-energy structure (or structures) of the cyclic molecule is valuable in providing a way of locating at least one *subset* of the low-energy structures of the linear chain, namely, the correlate structures. In going from cyclic to linear with the same number of residues, the end-to-end length must be large enough to relieve short contacts between atoms near the ends of the chain (Figure 1a). Now, as the length of the open chain is increased beyond the size of the cyclic molecule, the correlate structure will have to be further optimized to provide favorable interactions between successive turns of the resulting helix. In this respect it is fortunate that the X-ray structure of *cyclo*-(VPGVG)$_3$ turns out to be useful. The crystal structure of this molecule shows[7] that each cyclic molecule has threefold symmetry, consistent with the NMR data.[8] The threefold symmetry axis coincides with one of the crystal axes; that is, the cyclic molecules stack on top of one another along the symmetry axis with a spacing of 10 Å. This is indeed interesting, since the interaction between successive cyclic molecules suggests a favorable interaction between successive turns of the correlate helix (Figure 2). The interactions between turns may also result in the preferential stability of one handedness over the other. It will be of interest to obtain conformational energies of helices of each handedness by energy minimization techniques, starting with correlate structures of the types shown in parts b and c of Figure 1.

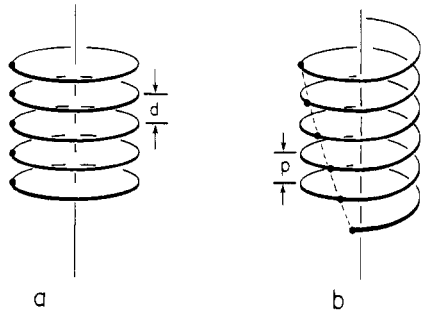

Figure 2. Schematic comparison of a one-dimensional lattice of cyclic molecules (a) with a helical structure (b) derived from its linear correlate. The helical structure may have a nonintegral repeat and this is illustrated in (b). The situation seen in (a) is found in the crystal structure of *cyclo*-(VPGVG)$_3$. An examination of the interaction between neighboring cyclic molecules in the crystal structure will be useful in constructing the helical structure of (VPGVG)$_n$ with the optimum pitch p resulting in similar interturn interactions.

Mathematical Description of a Cyclic Conformation and Linear Helical Conformations

A systematic repetition of a sequence of backbone torsion angles,[9] (ϕ_i, ψ_i), with i = 1–N, results in a helical conformation, with the helical monomer unit being composed of N residues. This monomer unit of the helix should contain an integral number of residues. The resulting helical structure is also characterized by a pair of helical parameters: n, the number of helix monomers per turn ($n \times N$ being the number of residues per turn), and h, the axial translation per helix monomer. The pitch of the helix is therefore $n \times h$. The helical parameters and the radii of the helix for the various atoms can be readily calculated from bond lengths, bond angles, and torsion angles.[10-12] The converse problem of computing all the torsion angles (and hence the conformation) from given values of helical parameters is less straightforward. This problem may, however, be solved by a simple generalization[13] of the Gō–Scheraga solution of the cyclization condition.[14,15] This is possible since n-fold symmetric cyclic structures are special cases of linear helical conformation: the linear helix becomes an n-fold symmetric cyclic molecule under the limiting conditions of $h \rightarrow 0$, $n \rightarrow$ integer. Thus, on relaxing the cyclization conditions in the Gō–Scheraga solution[15] by allowing h to be nonzero and n to be nonintegral, we obtain the helix conditions. The general mathematical method of solving the helix conditions has already been described by Gō and Okuyama.[13]

Details of the Calculations

Using standard bond lengths, bond angles, and planar peptide units, the (ϕ, ψ) torsion angles at the residues Val$_1$, Pro$_2$, Gly$_3$, and Val$_4$ were varied in intervals of 5° over a span of ±30° about the values found in one of the minimum-energy structures[8] for *cyclo*-(VPGVG)$_3$ having a conformation quite similar to the one found in the crystal[7] (see Table I). For each set of these torsion angles, the Gō–Scheraga helix conditions were solved by using a method similar to that given by Gō and Okuyama[13] to determine the appropriate values for (ϕ, ψ)(Gly$_5$) corresponding to the helical parameters in the region n = ±2.5–3.5 and h = 2.5–4 Å. This choice of helical parameters results in helices with a pitch close to the 10-Å repeat found in the crystal structure of *cyclo*-(VPGVG)$_3$ (see Figure 2). For the resulting helices, conformational en-

Table I
Torsion Angles (Deg) of the Low-Energy β Spirals of $(VPGVG)_n$ Compared with Those of *cyclo*-$(VPGVG)_3$

residue	torsion angle	minimum-energy[a] conformation of *cyclo*-$(VPGVG)_3$	right-handed β spiral A	left-handed β spiral B
Val_1	φ	−112	−120	−109
	ψ	115	105	107
Pro_2	φ	−58	−60	−60
	ψ	118	120	120
Gly_3	φ	111	120	135
	ψ	−58	−40	−42
Val_4	φ	−95	−120	−90
	ψ	95	80	75
Gly_5	φ	−180	−153	−101
	ψ	−178	−132	34
n (no. of pentamers per turn)		3	2.7	−2.7
h, Å		0	3.5	3.4
pitch, Å		0	9.45	9.18
energy, kcal/mol of pentamer		*b*	0	2.10
radius, Å				
outermost C^α			5.99	7.06
outermost side-chain carbon			8.24	8.28

[a] Corresponds to the minimum-energy structure C of Table IV of ref 8. [b] The energy of the cyclic molecule cannot be readily compared with those of the β helices: certain covalent linkages present in the cyclic structure are obviously not present in the helices; also, helices have been taken to be infinitely long.

ergies were obtained by using the energy functions of Momany et al.[16,17]

Results and Discussion

The calculations resulted in many low-energy helical structures with a pitch of about 10 Å. The torsion angles of the two typical minimum-energy helices A and B are reported in Table I. The stereoperspective ORTEP plots of these helices are given in Figures 3 and 4. The structure of Figure 3 (structure A) is a right-handed helix, while that of Figure 4 (structure B) is left-handed.

Structure A shows an interesting conformation. The Pro_2-Gly_3 β-turn segment is roughly parallel to the helical axis. The β turns therefore play the role of "spacers" between successive turns of the helix. As one goes along the peptide sequence, the chain periodically moves up and down along the helical axis; the down movement occurs at the β turn while the segment Val_4-Gly_5-Val_1 produces the upward shift. This may be seen more clearly in Figure 3b, where only C^α atoms of the structure have been delineated. There are no hydrogen bonds between turns. The interaction between turns is well optimized with Pro_2 occurring above a Gly_5 and a Gly_3 above a Val_1. All the hydrophobic parts occur essentially on the exterior surface of the helix. The open interior of the helix is accessible for solvent molecules from outside through the large "cavities" on the surface. These cavities are created by the upward movement of one turn stacking over a downward movement of the turn below. The nonintegral repeat of this helix inevitably creates several spiralling hydrophobic ridges on the surface. In particular, one can visualize a helical lipophilic band along the pentamer sequence $i, i + 3, i + 6, \ldots$ This band is a right-handed helix with a pitch of ~95 Å. As has previously been proposed,[18,19] the occurrence of each lipophilic band may have interesting implications on the nature of the interaction between two or more such β spirals, perhaps leading to the formation of a twisted filament.

In order to achieve a visual comparison between these helices and the cyclic correlate, similar stereoplots of *cyclo*-$(VPGVG)_3$ are shown in Figure 5. These plots correspond to one of the low-energy conformations[8] of the cyclic molecule (see Table I), a conformation similar to the one found in the crystal structure.[7] In fact, a "stack" of

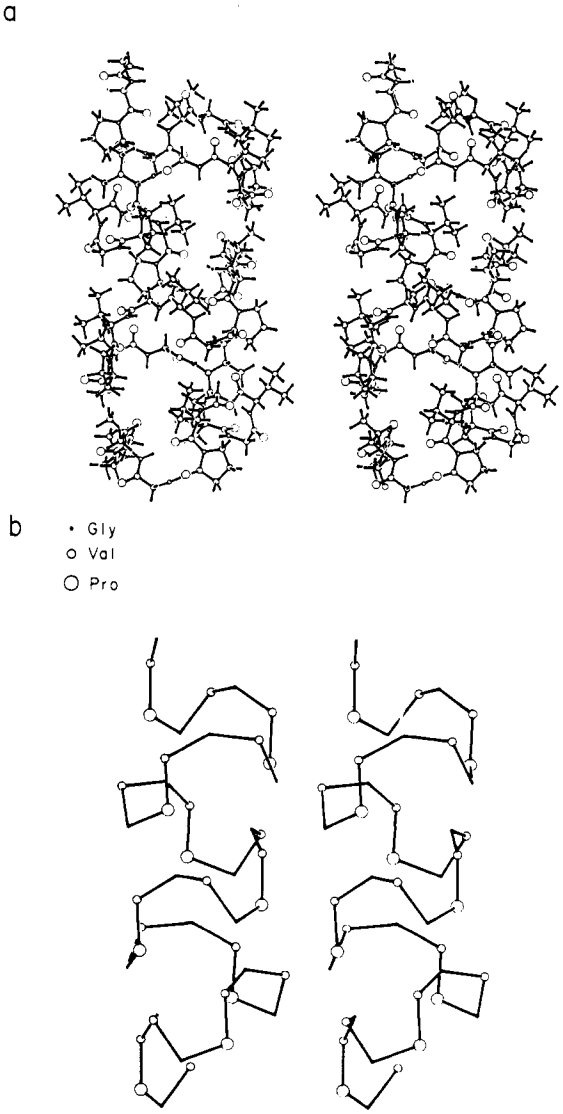

Figure 3. Stereoperspective plots of low-energy structure A of poly(pentapeptide) showing all atoms (a); only C^α atoms are shown in (b).

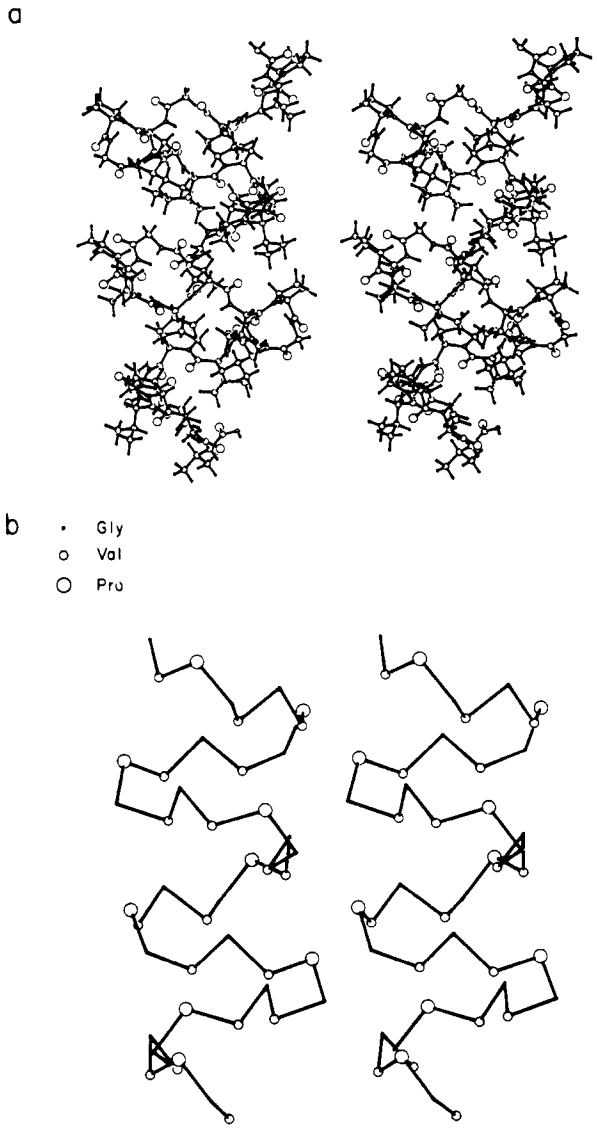

Figure 4. Same as Figure 3 for low-energy structure B.

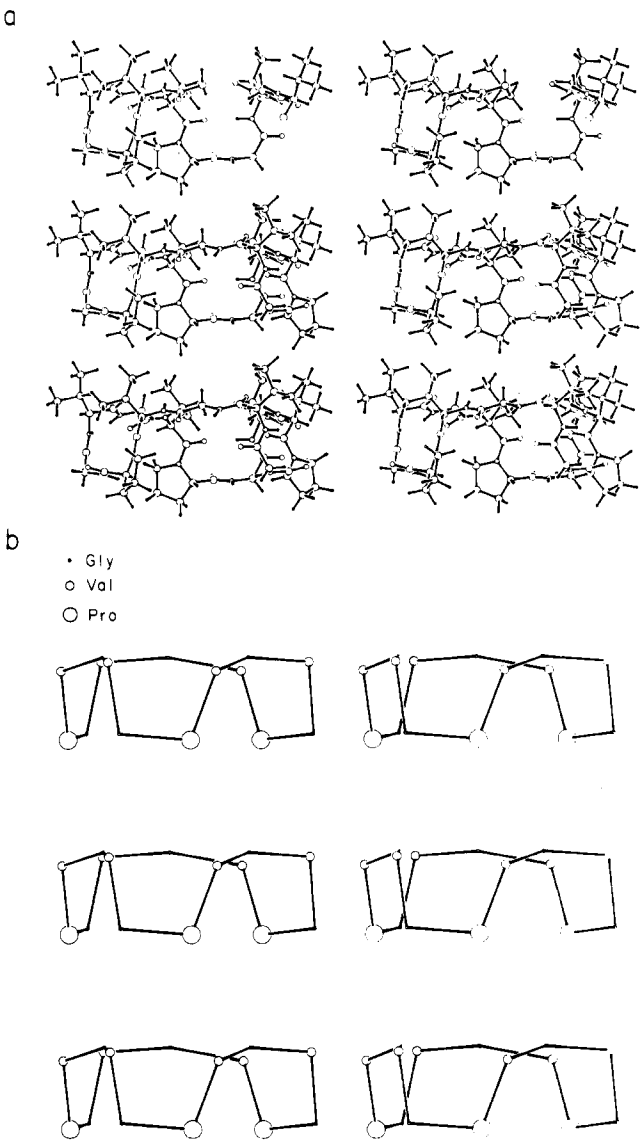

Figure 5. Stereoplots of a stack of *cyclo*-(VPGVG)$_3$ in a minimum-energy conformation similar to that found in the crystal structure. The spacing between the cyclic structures is 10.3 Å. The top molecule in (a) is not fully depicted.

cyclic molecules is shown (as in Figure 2a) with an axial spacing of 10.3 Å, corresponding to a minimum energy of intermolecular interactions in this stack for the chosen conformation of the cyclic molecule. The nature of the interactions seen between successive turns of the helix in Figure 3 and those existing between neighboring cyclic structures in Figure 5 is quite different. These differences are due to the change in n from 3.0 to 2.7 as one goes from the cyclic structure to the linear right-handed helix.

The torsion angles of structure A are given in Table I, where they may be compared with those of the low-energy conformation of the cyclic correlate *cyclo*-(VPGVG)$_3$. It may be seen that the angles are close to those of the cyclic molecule. Therefore, structure A is indeed a linear correlate of *cyclo*-(VPGVG)$_3$.

The left-handed helix, B, shown in Figure 4 displays quite a different arrangement of atoms. While the prolines occur on the outside, the valines are on the inside, giving a hydrophobic core. Thus, this is an oiled-coil.[3] The β-turn segment no longer functions as a spacer; rather the valyl side chains occurring near the helical axis perform this function. The turns are flatter, the disposition of the β-turn segments being nearly perpendicular to the helical axis, contrary to what is seen in the crystal structure of *cyclo*-(VPGVG)$_3$. It may be seen from Table I, that the torsion angles ϕ, ψ at Gly$_5$ are quite different for this structure, corresponding to a different class of Gō–Scheraga helix solutions. Though it is an energetically reasonable structure this cannot be viewed as a linear correlate of *cyclo*-(VPGVG)$_3$.

It may be noted that the difference in the torsion angle ϕ(Gly$_5$) between the right- and the left-handed β spirals will lead to different $\sum_i {}^3J(C^\alpha H_i\text{–}NH)$ coupling constants, namely, 8.5 Hz for the right-handed β helix and 15 Hz for the left-handed helix. A value of ~11 Hz is observed for poly(pentapeptide) in H_2O at 60 °C. Because the peptide moieties flanking the Gly$_5$ α carbon can exhibit large librations, it should not be expected that a single selected, lowest energy structure would correlate exactly with the solution $\sum_i {}^3J(C^\alpha H_i\text{–}NH)$ of Gly$_5$.

The right-handed β spiral derived as a linear correlate of the cyclic peptide *cyclo*-(VPGVG)$_3$ is very similar to the one proposed from NMR-derived secondary structural considerations[20] as the most ordered state that one would expect to obtain in the case of a single, isolated chain molecule of the poly(pentapeptide) dried from water at 60 °C. Though this is a limiting case, it is nevertheless a conceptually useful reference state. Indeed, the next step will be to consider the interaction between a pair or more

of such β spirals to obtain a low-energy twisted filament structure.

Acknowledgment. This work was supported in part by the National Institutes of Health, Grant No. HL-11310.

References and Notes

(1) See, for instance: Deber, C. M.; Madison, V.; Blout, E. R. *Acc. Chem. Res.* **1976**, *9*, 107.
(2) Urry, D. W. *Proc. Natl. Acad. Sci. U.S.A.* **1972**, *69*, 1610.
(3) Gray, W. R.; Sandberg, L. B.; Foster, J. A. *Nature (London)* **1973**, *246*, 461.
(4) Foster, J. A.; Bruenger, E.; Gray, W. R.; Sandberg, L. B. *J. Biol. Chem.* **1973**, *248*, 2876.
(5) Sandberg, L. B., private communication.
(6) Urry, D. W.; Trapane, T. L.; Sugano, H.; Prasad, K. U. *J. Am. Chem. Soc.* **1981**, *103*, 2080.
(7) Cook, W. J.; Einspahr, H.; Trapane, T. L.; Urry, D. W.; Bugg, C. E. *J. Am. Chem. Soc.* **1980**, *102*, 5502.
(8) Venkatachalam, C. M.; Khaled, M. A.; Sugano, H.; Urry, D. W. *J. Am. Chem. Soc.* **1981**, *103*, 2372.
(9) IUPAC–IUB Commission on Biochemical Nomenclature *J. Mol. Biol.* **1970**, *52*, 1.
(10) Ramakrishnan, C. *Proc. Indian Acad. Sci.* **1964**, *59*, 317.
(11) Sugeta, H.; Miyazawa, T. *Biopolymers* **1967**, *5*, 673.
(12) Ramachandran, G. N.; Sasisekharan, V. *Adv. Protein Chem.* **1968**, *23*, 283.
(13) Gō, N.; Okuyama, K. *Macromolecules* **1976**, *9*, 867.
(14) Gō, N.; Scheraga, H. A. *Macromolecules* **1970**, *3*, 178.
(15) Gō, N.; Scheraga, H. A. *Macromolecules* **1973**, *6*, 273.
(16) Momany, F. A.; Carruthers, L. M.; McGuire, R. F.; Scheraga, H. A. *J. Phys. Chem.* **1974**, *78*, 1595.
(17) Momany, F. A.; McGuire, F. F.; Burgess, A. W.; Scheraga, H. A. *J. Phys. Chem.* **1975**, *79*, 2361.
(18) Urry, D. W.; Long, M. M. "Elastin and Elastic Tissue"; Plenum Press: New York, 1977. *Adv. Exp. Med. Biol.* **1977**, *79*, 685.
(19) Urry, D. W. *Perspect. Biol. Med.* **1978**, *21* (2), 265.
(20) Urry, D. W.; Long, M. M. *CRC Crit. Rev. Biochem.* **1976**, *4*, 1.

Conformational Entropy Effects in a Compressible Lattice Fluid Theory of Polymers

K. M. Hong* and J. Noolandi*

Xerox Research Centre of Canada, 2480 Dunwin Drive, Mississauga, Ontario, Canada L5L 1J9. *Received March 2, 1981*

ABSTRACT: An earlier theory of an incompressible multicomponent system consisting of both polymers and small molecules has been modified to account for free-volume effects by taking one of the small-molecule components to be vacancies. The resulting equation-of-state theory, based on the lattice fluid model, correctly accounts for conformational entropy effects, which have been neglected by Poser and Sanchez. The theory is applied to the calculation of the surface tension of pure polymer melts, and good agreement with experiment is obtained.

1. Introduction

The equation-of-state approach to the study of polymer liquids developed by Flory and co-workers[1-4] has enjoyed great success in describing the thermodynamical properties and the phase separation behavior of polymer systems. Such phenomena as the lower critical solution temperature (LCST) behavior can be understood in terms of the equation-of-state theory whereas the older Flory–Huggins theory completely fails to describe it. A more recent version of an equation-of-state theory, based on a lattice fluid model and capable of describing both the liquid and the vapor phases, has also been advanced by Sanchez and Lacombe.[5-9]

Recently, based on a functional integral approach due to Helfand,[10] we have developed a theory for an inhomogeneous incompressible liquid consisting of both polymers and small molecules.[11] In the limit of a homogeneous system, it reduces to the Flory–Huggins theory and hence suffers from the same drawbacks, although it should be noted that for many practical applications the Flory–Huggins theory is still useful, provided the interaction parameters are used in a phenomenological sense. Nonetheless it would be desirable to have a generalization of the equation-of-state theories to describe inhomogeneous systems. Such a step has been taken by Poser and Sanchez,[9,12] who use the lattice fluid model in conjunction with the theory of Cahn and Hilliard[13] to study the interfacial properties of liquids. However, in so doing, they have neglected conformational entropy effects which are important, especially when incompatible polymer blends are involved.

The purpose of this paper is to demonstrate that our formalism[11] for an incompressible multicomponent system can easily be modified to take into account free-volume effects simply by taking one of the small-molecule components to be vacancies. Then the theory yields the equation of state of the lattice fluid model, while at the same time conformational entropy effects are properly taken care of.

In section 2 we present a reformulation of our theory and derive an expression for the interfacial tension. In section 3, we obtain the equation of state and identify the various parameters used in the theory. The theory is then applied to calculate the surface tension of some polymer liquids and the results are discussed in section 4.

2. Lattice Fluid Model

As described in detail in ref 11, the partition function $\mathcal{Z}$ of a multicomponent fluid can be written as a functional integral over the density ρ_i and effective field ω_i of the various components; viz.

$$\mathcal{Z} = \mathcal{N} \int (\prod_i^0 \delta\rho_i(\cdot)\delta\omega_i(\cdot)) \exp(-\mathcal{F}/k_B T) \qquad (2.1)$$

Here $\mathcal{N}$ is a normalization constant and a "0" over the product or summation sign indicates that the term $i = 0$ (describing vacancies) is included in the product or sum. $\mathcal{F}$ is the functional

$$\mathcal{F}(\{\rho_i(\cdot),\omega_i(\cdot)\}) = \int d^3r \left\{ f - \frac{1}{12}\sum_{ij} W_{ij}\sigma_{ij}^2 \vec{\nabla}\rho_i(\mathbf{r})\cdot\vec{\nabla}\rho_j(\mathbf{r}) - \sum_i^0 \rho_i(\mathbf{r}) \left[\omega_i(\mathbf{r}) + \frac{k_B T}{Z_i} \ln\left(\frac{\rho_i(\mathbf{r})\mathcal{Q}_i}{N_i}\right)\right]\right\} \qquad (2.2)$$

$$f(\{\rho_i(\mathbf{r})\}) = \frac{1}{2}\sum_{ij} W_{ij}\rho_i(\mathbf{r})\rho_j(\mathbf{r}) + k_B T \sum_i^0 \frac{\rho_i(\mathbf{r})}{Z_i} \ln\left(\frac{\rho_i(\mathbf{r})}{Z_i z_i e}\right) \qquad (2.3)$$

0024-9297/81/2214-1229$01.25/0